ISSN 1 746-7233, England, UK
World Journal of Modelling and Simulation
Vol. 8 (2012) No. 3, pp. 231-240

Lumped parameter electromagnetic modelling approach for transient analysis in EHV transformers

Dilip Debnath[1*], Abhinandan De[2], Abhijit Chakrabarti[3]

[1] School of Electrical Engineering, VIT University, Vellore-632014, India
[2] Department of Electrical Engineering, Bengal Engineering & Science University, Howrah 711103, India
[3] Jadavpur University, Kolkata 700032, India

(*Received January 10 2011, Accepted March 26 2012*)

Abstract. This paper presents a novel lumped parameter high frequency circuit model of transformer using EMTP analysis of transients within the windings. The model which has been developed based on transformer geometry, configuration and design parameters, can adequately reproduce the frequency response characteristics of the original transformer. The response characteristics of the EMTP model presented in this work has been validated with the original transformer's laboratory test results. The behavioural responses of the windings were studied under 1.2/50 μs standard lightning impulse and fast-front switching surge. It has been observed that the developed model successfully reproduced the windings response under these transients and the results indicate that the voltage stresses developed on the winding insulation are marginally higher under fast-front switching surge as compared to standard lightning impulse.

Keywords: EHV transformer, EMTP, fast-front switching surge, frequency response

1 Introduction

The rate of internal insulation failure of grid connected EHV transformers is quite high. This has prompted the authors to investigate the possible reason for insulation failure in EHV transformers connected to EHV power grids. The studies got more relevance when a series of dielectric failure in several large EHV transformers were reported on the American Electric Power (AEP) System[9, 11]. The matter received considerable attention within the IEEE Transformer Committee and a working group was formed to investigate the phenomena involved. Diagnostic investigations inferred that the failures were initiated either by switching actions in the grid or due to system faults which triggered internal natural resonance frequencies of the windings of the transformer. Thereafter many researchers have tried to develop high frequency models of EHV transformer to study the frequency response and the distribution of transient high voltages in transformer windings to assess the accurate voltage stresses that are likely to occur under surge conditions. Accordingly, the insulation structure for the windings is decided. High-voltage large power transformer windings are much complicated systems than simple single layer coil systems. Mathematical modelling of such a complicated system is difficult without simplifying assumptions. Moreover, the transient response of transformers depends on many factors, like the type of winding, the manner in which the windings are subjected to surge, how other windings are connected, whether the grounding of windings are solid or through resistance, the degree of non-homogeneity in the windings due to local reinforcement of the turn insulation, etc. In this paper, a modelling technique for transformer windings has been developed with concentrated resistances, inductances and capacitances that simulate the electrical properties and a suitable numerical method of analysis utilizing circuit solution principles has been developed. The major contribution of this paper is the simple but accurate approach towards high frequency modelling of EHV transformer windings which can faithfully reproduce the

* Corresponding author. Tel.: +91-4162204201. *E-mail address*: d.dn@ovi.com.

transient characteristics of the transformer. The techniques developed in computing the lumped inductance, capacitance and resistance of the winding disk coils are the original contributions of the authors and are simple to adopt. The other important contribution of the paper is the thorough analysis and comparison of the winding insulation stresses under standard system transients like lightning and switching. The results of this study should be useful for the transformer designers to assess and evaluate the magnitude of insulation stresses in transformers under such operating conditions. This paper is organised as follows: In Section 2, development of equivalent circuit model for transformer has been explained with design data. The consideration for computation of model parameters has been given in Section 3. In Section 4, development of EMTP model of the transformer has been discussed. The developed EMTP model has been validated with the experimental frequency response in Section 5. Frequency response of 400 kV main and tap changer windings have been analysed in Section 6. In Section 7, voltage stress under standard lightning impulse and fast-front switching surge has been compared. Finally, in Section 8, conclusion has been drawn about the accuracy and validity of the model. Future scope of work is also included in Section 8.

2 Development of equivalent circuit model for transformer

The equivalent circuit is developed on the assumption that the winding terminals are connected as per IEC specification during impulse tests[1]. Based on transformer geometry and configuration, a lumped parameter high frequency circuit model[5, 15, 17] of the concerned 31.5 MVA, 400/220/33 kV transformer has been developed.

The developed equivalent circuit model contains 78 elementary sections, representing 46 main and 32 tap winding disks. The following design data of the grid connected three-phase, 31.5 MVA, 400/220/33 kV; Ynd11 transformer with tap changer winding has been used to calculate lumped parameters for the model.

Table 1. Design data: 400 kV Winding details

Main winding	Tap winding
Type of winding: Interleaved continuous disk	Type of winding: Interleaved continuous disk
Number of parallel paths: 1	
Number of disks: 46	Number of disks: 32
Turns per disk: 24	Turns per disk: 18
Separation between disks:	Separation between disks:
(i) 8mm between interleaved disk pairs	(i) 6mm between interleaved disk pairs
(ii) 12mm between two successive interleaved groups	(ii) 8mm between two successive interleaved groups

3 Computation of model parameters

Computation of model parameters is based on available design data and relevant dielectric and other properties of the insulating materials used in the design. Detailed computation methods followed in the determination of various model parameters have been presented in the Appendix section of the paper. Only a summary of these computational methods are discussed in this section.

(1) Determination of Series capacitance of each coil

Inter-turn as well as inter-disk series capacitances[3, 10] between adjacent coils have been taken into consideration. However, small stray capacitances between one coil to other distant coil have been neglected.

(2) Determination of Shunt capacitance between coils and neighboring earthed bodies

Shunt capacitance between coils and neighboring earthed bodies, that include both the metal tank as well as non-impulse windings, have also been calculated.

(3) Determination of Shunt capacitances between different winding sections

Electrostatic coupling between the main as well as tap windings has been considered separately to determine shunt capacitances between different winding sections.

Table 2. Design data: Disc coil dimensions

	400 kV Main winding	Tap winding
Mean radius	650 mm	830 mm
Radial width	87.7 mm	32.9 mm
Axial height	16.2 mm	14.6 mm
Conductor width	2.4 mm	2.2 mm
Conductor height	14.9 mm	12.6 mm
Thickness of paper insulation	0.75 mm	0.6 mm

(4) Determination of Self and Mutual inductance of the coils

Self-inductance of the disk coils has been calculated using Grover's extension to Rosa's formula for computation of self inductance of circular disk coils of rectangular cross-section[2]. Mutual inductance between the disk coils has been calculated by "Lyle method of Equivalent Filament"[12], and the tables presented by Grover [8]. In a lumped parameter transformer model, representation of evenly distributed numerous mutual inductances formed by each coil with the other coils is virtually impossible. Such distributed mutual inductances have been lumped together to form a single equivalent mutual inductance[6]. Then after considering inductive coupling between the windings, mutual inductances between different distinct winding sections (which are not too far away e.g. main and tap windings) has been calculated.

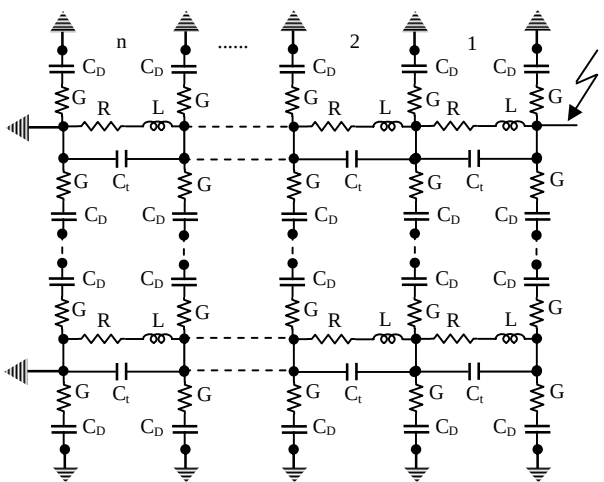

Fig. 1. Part of the n section circuit model of 400/220/33kV transformer developed for the study

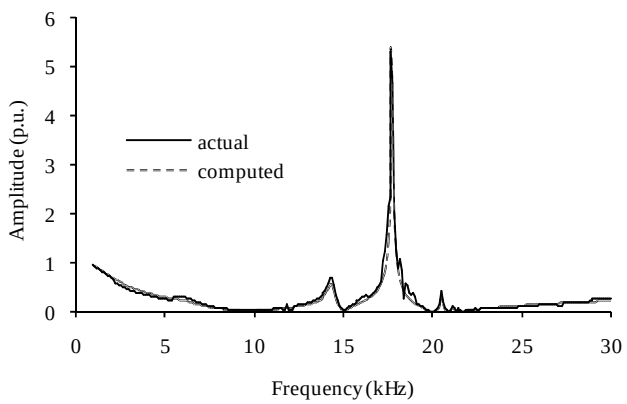

Fig. 2. Transfer function (winding admittance) frequency response

All the inductance components have finally been lumped together to an easily representable form of "equivalent inductance per disk coil" using the method suggested by K. A. Wirgau [18]. The validity and accuracy of the proposed modelling technique has been established in [3, 4].

5. Determination of Equivalent series resistance (R) *of the coils*

Effective resistance of the coils has been calculated, considering non-uniform distribution of current in the conductors due to skin effect and eddy currents[13, 14, 16]. However parallel resistances, representing dissipation losses in the capacitor dielectrics, and eddy current losses formed by low voltage winding in the conducting cylinder have been neglected.

4 Development of EMTP model for 400 kv winding

After computation of the parameter values, EMTP (Electromagnetic Transient Programming) has been used to simulate and analyze the frequency response characteristic of the transformer. Also, the impact of standard 1.2/50 μs lightning impulse and fast-front switching surges on the windings have been studied and compared. A part of the developed EMTP model containing n number of identical sections has been shown in Fig. 1.

5 Validation of the developed EMTP model

An example has been added here to demonstrate accuracy of the proposed modelling technique and to establish validity of the results presented subsequently in this paper. The incident lightning impulse voltage and corresponding neutral current wave of the transformer were recorded in the HV test laboratory during lightning impulse test on the actual transformer. These data have been utilized to obtain frequency responses of the whole transformer (neutral current/applied impulse voltage). The results obtained from the developed EMTP model closely match with the response characteristics of the original transformer, showing similar resonance peak and cross over, as shown in Fig. 2.

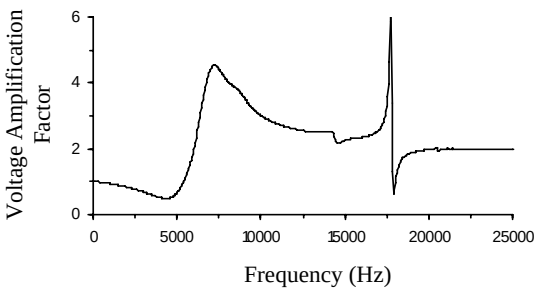

Fig. 3. Frequency response of a group of 20 disk-coils of 400kV winding

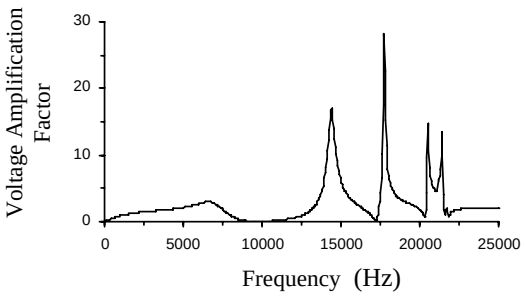

Fig. 4. Frequency response of a group of 20 disk-coils of tap winding

The agreement between the computed and actual frequency response characteristics, both in amplitude and frequency, establishes accuracy of the developed model.

6 Frequency response of 400 kv main and tap changer windings

The frequency responses of the main and tap winding disk coils on the 400 kV side of the transformer have been determined by analyzing the developed circuit model using Electromagnetic Transient Programming (EMTP). To determine the frequency responses of windings, each phase of the transformer has been excited at its terminals by $400/\sqrt{3}$ kV (rms) variable frequency sinusoidal voltage source. The responses obtained from ATP simulation have been shown in Fig. 3 and Fig. 4. The voltage amplification in the coils

has been presented in per unit (pu) values as multiples of the nominal coil voltage under power frequency operation.

The frequency response of the group of 20 disk coils of the 400 kV main winding of the transformer shows one single major resonance around 7.2 kHz with voltage amplification factor of about 4.5 (Fig. 3). This signifies that excitation at the transformer terminal at this frequency would force internal resonance in the main winding coils and theoretically produce internal over voltage of magnitude as high as 4.5 times the nominal voltage experienced by these coils under normal power frequency operation. The tap winding on the other hand exhibits four major resonances at 14.4 kHz, 17.7 kHz, 20.3 kHz and 21.5 kHz with still higher voltage amplification factors in the range 12-29 (Fig. 4).

7 Comparison of voltage stress under standard lightning impulse and fast-front switching surge

Transformers are subject to standard high voltage dielectric insulation tests during their manufacture. Such tests replicate the aperiodic voltage wave forms, which the transformers are likely to experience during their operation. Standard aperiodic waveforms do not necessarily represent the most disastrous voltage stress condition which the transformer could actually experience during service. It is quite possible that the voltages generated within the system could produce even more unfavorable voltage stress condition to some transformers in certain systems. It is thus necessary to ascertain how the winding stresses under system originated voltages compare with the voltage stresses produced by standard aperiodic laboratory test waves.

(1) Response under Standard Lightning Impulse

Response of the transformer's 400kV winding under 1.2/50 μs standard lightning impulse[7] has been shown in Fig. 5. The peak voltage across the group of 20 disk coils of the 400 kV main and tap windings are observed to be 40% and 9% of the applied terminal voltage respectively. No sign of resonance is visible from the diagram. This should be of great concern because line end coils are generally provided with the highest degree of insulation, as maximum stress on dielectric is anticipated at the line end under lightning impulse or steep-front aperiodic switching surge. Due to non-linear distribution of surge voltage in the windings, middle and end coils in general experience much lower stress and are generally provided with lower insulation to optimize cost.

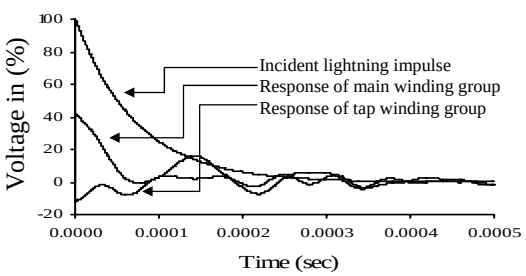

Fig. 5. Response of the windings under standard lightning impulse

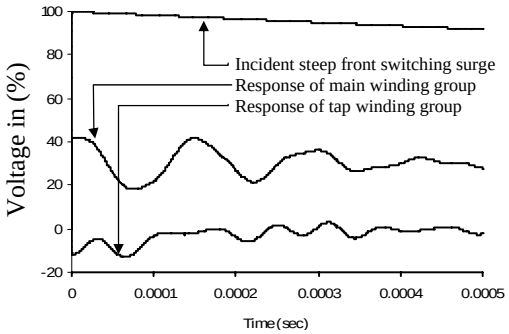

Fig. 6. Response of the windings under steep-front switching surge

(2) Response under Fast-Front Long-Tail Switching Surge

The authors have investigated how the same transformer would behave under 1.2/4000 μs steep-front long-tail switching surge. The results of the study shown in Fig. 6 indicate that steep-front long-tailed surge can stress windings to higher levels compared to lightning and slow rising switching surges. The peak voltage developed across the group of 20 disk coils of the 400kV main and tap windings under steep-front surge are observed to be 42% and 11% of the applied terminal voltage respectively which are marginally greater than the corresponding lightning impulse responses (Fig. 6). It is seen that due to broader spectrum of frequency

content, steep-front surges can excite windings at their natural frequencies and subject them to high stresses for longer duration of time.

8 Conclusion

A technique for modelling grid connected EHV transformers has been suggested for the analysis of winding's response to transients. A 31.5 MVA, 400/220/33 kV EHV transformer has been modelled in EMTP using the proposed modelling technique and the simulation results were compared with actual response of the transformer collected from the field for validation purpose. The developed model successfully reproduced the winding's frequency response characteristics. The behavioural response of the transformer under standard 1.2/50 μs lightning impulse as well as under fast-front switching surge have been studied and compared. The results indicate that the voltage stresses developed on the windings are marginally higher under fast-front switching surge as compared to standard lightning impulse. The results presented in the paper should be valuable for transformer designers as it carries important information regarding voltage stresses on winding insulation under transients. To make the results more exhaustive, future research work will be appreciated to assess windings response under other types of transient wave-forms like oscillatory switching transients, chopped lightning impulse wave etc. and the results can be compared to decide upon an effective and adequate insulation design for EHV transformers.

References

[1] *Power transformer—insulation levels and dielectric tests*, *3*, vol. 76. IEC Publication, 1970.

[2] P. Blanken. A lumped winding model for use in transformer models for circuit simulation. *IEEE Transaction Power Electron*, 2001, **16**(3): 445–460.

[3] A. De, N. Chatterjee. Part winding resonance: Demerit of interleaved high-voltage transformer winding. **in:** *IEE Proceedings-Electric Power Applications*, vol. 147, 2000, 167–174.

[4] A. De, D. Debnath, A. Chakrabarti. A study on the impact of low-amplitude oscillatory switching transients on grid connected ehv transformer windings in a longitudinal power supply system. *IEEE Transaction on Power Delivery*, 2009, **24**(2): 679–686.

[5] R. Degeneff, M. Vakilian. Modelling power transformers for transient voltage calculations. *Council on Large Electric Systems*, 1992, 12–304.

[6] F. Grover. *Inductance Calculation: Working Formulas and Tables*. Dover Publications, Inc., 1962.

[7] M. Jayaraju, I. Duat, M. Adzman. Impulse voltage generator modelling using matlab. *World Journal of Modelling and Simulation*, 2008, **4**(1): 57–63.

[8] T. Lyle, P. Mag. *Philosophical Magazine*, *3*, vol. 310. Taylor and Francis Ltd, 1902.

[9] M. Elroy. On the significance of recent ehv transformer failures involving winding resonance. *IEEE Transactions on Power Apparatus and Systems*, 1975, **PAS-94**(4): 1301–1316.

[10] A. Morched, L. Marti, J. Ottenvangers. A high-frequency transformer model for the emtp. *IEEE Transaction on Power Delivery*, 1993, **8**(3): 1615–1625.

[11] J. Phelps, A. Carlomagno. Experience with part-winding resonance in EHV auto-transformers: Diagnosis and corrective measures. *IEEE Transactions on Power Apparatus and Systems*, 1975, **PAS-94**(4): 1294–1300.

[12] E. Rosa. Calculation of the self-inductance of single-layer coils. *Bulletin of the Bureau of Standards*, 1906, **2**: 161–187.

[13] A. Sawheny. *A Course on Electrical Machine Design*. Dhanpat Rai & Sons Publishing Company, India, 1996.

[14] A. Singh, J. Marti, K. Srivastava. Circuit reduction techniques in multiphase modelling of power transformers. *IEEE Transaction Power Delivery*, 2010, **25**(3): 1573–1579.

[15] A. Soyal. A method for wide frequency range modelling of power transformer and rotating machines. *IEEE Transactions Power Delivery*, 1993, **8**(4): 1802–1810.

[16] R. Stoll. *The Analysis of Eddy Currents*. Clarendon Press, Oxford, 1974.

[17] P. Vaessen. Transformer model for high frequencies. *IEEE Transactions Power Delivery*, 1988, **3**(4): 1761–1768.

[18] K. Wirgau. Inductance calculation of an air-core disk winding. *IEEE Transactions on Power Apparatus and Systems*, 1976, **PAS-95**(1):394–400.

Appendix

Details of the computational methods used in calculating model parameters

1. Self Inductance of Disk Coils

The formula used here applies to thick coils of disk shape for which the radial dimension is considerably greater than the axial dimension[2, 12].

The equivalent self-inductance is given by:

$$L = L_s - 0.004 \times \pi \times N \times a\,(G_1 + H_1)\,,$$

where,

$$L_s = 0.001 \times N^2 \times a \times P\mu H(\text{a is in cm}),$$
$$P = 4\pi \left[\left(\ln \frac{8a}{c} - 0.5 \right) + \frac{1}{24} \left(\frac{c}{2a} \right)^2 \times \left(\ln \frac{8a}{c} + 3.583 \right) \right].$$

All other nomenclatures are given along with the Fig. 7.

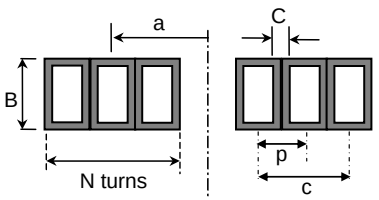

a = Mean radius of a disk coil
p = Winding pitch
C = Thickness of insulation between adjacent turns
B = Height of the insulated conductor
N = Number of turns in a disk coil
c = N_p = Approximate radial width of a disk coil

Fig. 7. Schematic of disk coil

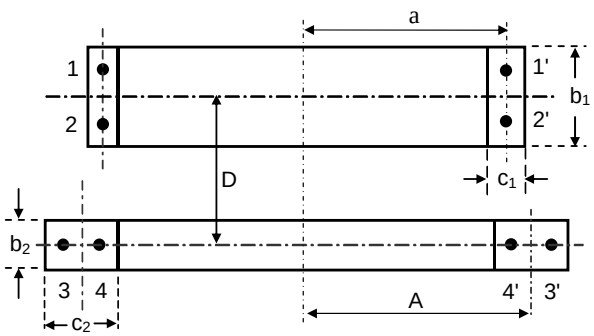

Fig. 8. Reduction of coils to equivalent filaments

2. Mutual-inductance between the elements

The mutual inductance between two co-axial circular filaments of negligible cross-sectional area, and radii a and A respectively, separated by distance d between their planes is found to be dependent upon the two parameters: a/A and d/A, and is given by the Eq. (1).

$$M = f\sqrt{Aa} = fA\sqrt{a/A}\mu H, \tag{1}$$

in which f is obtained from [12].

The formulae given above however apply only to circular filaments of negligible cross-section.

Lyle method of equivalent filaments

This is very accurate method for co-axial coils of dimensions such that the 4^{th} order and further higher order differential co-efficients in Taylor's series expansion are negligible. The dimensions of equivalent filaments in a general case is illustrated by Fig. 8, which shows two circular coils of rectangular cross-sections of mean radii a & A, axial dimensions b_1 & b_2, radial dimensions c_1 & c_2, having number of turns N_1 & N_2 and spacing of median planes D. *Lyle method* replaces the 2 coils by 4 equivalent filaments. Each filament is assumed to have half the number of turn of its coil. If the axial cross-sectional dimension $b_1$is greater than radial c_1, filaments 11' and 22' will have an equivalent radius r_1 slightly larger than the mean radius a, and the two filaments are located at an axial distance β on either side of the median plane. The defining equations for $r_1$and β are:

$$r_1 = a\left(1 + \frac{c_1^2}{24a^2}\right), \quad \beta = \sqrt{\frac{(b_1^2 - c_1^2)}{12}},$$

If, on the other hand, the second coil has its radial dimension c_2 greater than axial b_2, the coil is to be replaced by two co-planer circular filaments 33' and 44' located at the median plane but having equivalent radii $(r_2 + \delta)$ and $(r_2 - \delta)$ respectively, where:

$$r_2 = A\left(1 + \frac{b_2^2}{A^2}\right).$$

The mutual inductance between the two coils is then given by the formula:

$$M = N_1 N_2 \left(\frac{M_{13} + M_{14} + M_{23} + M_{24}}{4}\right),$$

The mutual inductance between the filaments is calculated by Eq. (1).

The table, used for the calculation of mutual inductance between two coils is as follows:

Table 3. Design data: Disc coil dimensions

Filaments	Product of turns	Radii	Axial spacing
11' & 33'	$(N_1 \times N_2)/4$	r_1 and $(r_2 + \delta)$	$D + \beta$
11' & 44'	$(N_1 \times N_2)/4$	r_1 and $(r_2 - \delta)$	$D + \beta$
22' & 33'	$(N_1 \times N_2)/4$	r_1 and $(r_2 + \delta)$	$D - \beta$
22' & 44'	$(N_1 \times N_2)/4$	r_1 and $(r_2 - \delta)$	$D - \beta$

Determination of the equivalent inductance of a coil

Assuming a section of the winding have n number of identical coils each of self-inductance L and mutual inductances Mi between two pairs of coils, where i indicates the number of coils away from the reference coil, the equivalent inductance of the whole winding section is given by the formula:

$$L_{eq} = n \times L + 2\sum_{i=1}^{n-1} (n - i) \times M_i.$$

Moreover, for two distinct winding sections, which are not too far away from each other, (for e.g. Main and Tap changer winding of a transformer) mutual inductances among the elements of two windings should also be taken into consideration. This method originally proposed by Wirgau [4] has been used in the present case. It replaces all the elements within one winding section by an equivalent lumped element. The proposed method has been illustrated in Fig. 9. Here two winding sections have been considered. The first having X number of elements with each of N_1 number of turns, and the second one having Y number of sections with each of N_2 number of turns have been replaced by equivalent lumped elements of XN_1 and YN_2 number of turns respectively. Distance D between the elements is same as the distance of separation of the central elements of the two winding sections.

3. Series Capacitance of Interleaved disk coils

In the calculation of series capacitance, inter-turn as well as inter-disc capacitances between adjacent coils have been taken into consideration [6, 18]. However small stray capacitances between one coil to other distant coils have been neglected.

Series capacitance of a disk coil is composed of two parts, being the resultant of: Inter-turn Capacitance and Inter-disc Capacitance.

1. Inter-turn Capacitance C_t

Since C_t depends upon the common area between two adjacent turns, which again depends upon diameter of the concerned turns, therefore, C_t does not have a constant value and changes with the turn diameter. So, for practical calculations, value of C_t at the mean turn of a disk coil has to be calculated.

Value of C_t at the mean turn is given by:

$$C_t = \frac{\pi D_m \left(h + 2\delta_t\right) \varepsilon_0 \times \varepsilon_{paper}}{2\delta_t},$$

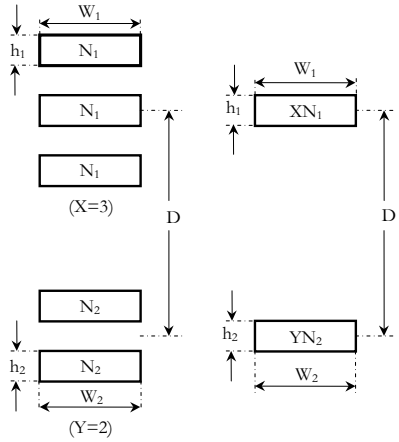

Fig. 9. Mutual Inductance between two distinct winding sections

where (refer Fig. 10),

H = Bare conductor height, t = Thickness of paper insulation, D_m = Diameter of mean turn, $\varepsilon_{\text{paper}}$ = Relative permittivity of paper = 3.5.

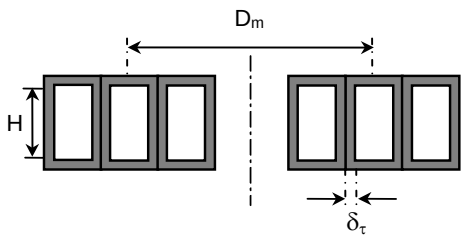

Fig. 10. Conductor arrangement in a disk coil

It is to be noted that in the calculation of common area between the turns, twice the thickness of paper insulation $(2\delta_t)$ has been added to bare conductor height to take into account the effect of flux fringing and stray capacitances.

Inter-disk Capacitance C_D

Inter-disk capacitance is calculated using the formula for capacitance between two parallel plate electrodes separated by composite dielectric of paper, press-board and oil, in the form as shown in Fig. 11. Assuming 35% of the common area between the coils being covered by press-board insulation and remaining 65% of the area being covered by oil, resultant inter-disk capacitance between two adjacent disk coils is expressed as:

$$C_D = \frac{\pi}{4}\left(D_0^2 - D_i^2\right) \times \varepsilon_0 \left[\left(\frac{0.35}{\frac{2\delta_t}{\varepsilon_{paper}} + \frac{\delta}{\varepsilon_{p.b}}}\right) + \left(\frac{0.65}{\frac{2\delta}{\varepsilon_{paper}} + \frac{\delta}{\varepsilon_{oil}}}\right)\right],$$

where, D_o = Outer diameter of disk coil, D_i = Inner diameter of disk coil, δ_t = Thickness of paper insulation, δ = Thickness of dielectric between coils, i.e. inter-disk separation, ε_{paper} = Relative permittivity of paper = 3.5, $\varepsilon_{p.b}$ = Relative permittivity of press-board = 4.0, ε_{oil} = Relative permittivity of oil = 2.22.

4. Equivalent high frequency resistance of the disk coils

Fig. 12 shows a case of subdivided (laminated) conductors placed in iron slot. It is assumed that the conductor is divided in N layers, each of height h_1, width b and length L. Total height of all the layers is $h = Nh_1$.

The average loss ratio for N layers is given by:

$$K_{e(average)} = \frac{R_{ac}}{R_{dc}} = 1 + (\alpha h_1)^4 \times \frac{N^2}{9},$$

where, $R_{d.c}$ is the d.c. resistance and $R_{a.c}$ is the equivalent resistance at high frequency, considering skin effect, and

$$\alpha = \sqrt{\frac{\pi \mu_0 b f}{\rho w}},$$

where, f is frequency and ρ is the resistivity of the conductor.

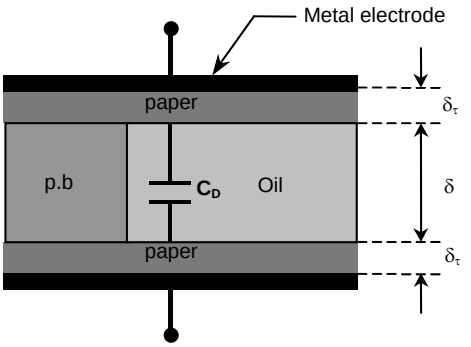

Fig. 11. Composition of Inter-Disk Capacitance

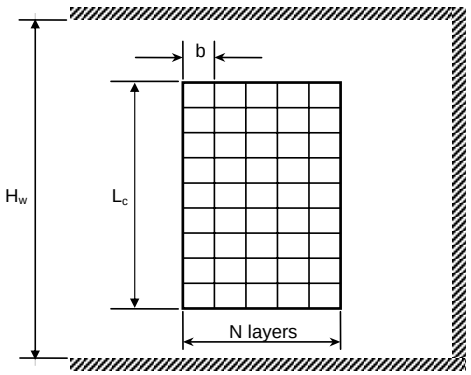

Fig. 12. Transformer winding inside the tank

The above generalized expression can be extended for a transformer winding, if each winding of axial height L_C can be considered to be located in a slot of width H_w, which is the height of the transformer window.